Supplemental Data

A systematic survey of *in vivo* obligate chaperonin-dependent substrates

Kei Fujiwara, Yasushi Ishihama, Kenji Nakahigashi, Tomoyoshi Soga,

and Hideki Taguchi

Supplemental Experimental Procedures

Plasmids

The plasmid pMCS (Fujiwara & Taguchi, 2007), in which the T7 promoter region of the plasmid pET15b(+) (Novagen) was replaced with the *tac* promoter, was used for constructing all plasmids. To construct plasmids for overexpression, fragments encompassing each full-length gene were amplified by PCR from *E. coli* K12 MG1655 chromosomal DNA. The amplified fragments were digested with NdeI/XhoI or NdeI/SalI. Each digested fragment was ligated into pMCS digested with NdeI/XhoI. The amplified genes with NdeI sites were partially digested to obtain the full-length genes. The C-terminal HA-tagged sequences were constructed by replacing the terminal codon sequence with either GGATCC or AGATCT. Fragments digested by NdeI/BamHI or NdeI/BglII were ligated into modified pMCS, in which an XhoI site was replaced by a sequence encoding the HA-tag (GGATCCTACCCATACGACGTCCCAGACTACGCTTAACTCGAG). The nucleotide-sequences of all constructed plasmids were verified.

Bioinformatics

Annotations of cytosolic proteins, functions, folds, and superfamilies were according to GenoBase (http://ecoli.naist.jp/GB6/search.jsp), except for the folds and functions of the Class III^{-} and Class IV proteins. Annotations of Class III^{-} and Class IV were according to either the SCOP database (http://scop.mrc-lmb.cam.ac.uk/scop/) or Kerner's results for folds (Kerner et al, 2005), and Ecocyc (http://ecocyc.org/) for functions. Essentiality for *E. coli* viability was according to GenoBase (http://ecoli.naist.jp/GB6/search.jsp). pI values were determined according to the ExPasy Compute PI/MW tool (http://ecoli.naist.jp/gb6/Resources/deletion/deletion.html). Hydrophobicities were calculated by the Kyte-Doolittle method (Kyte & Doolittle, 1982).

Proteomics

For the proteome analysis, 1.6 OD_{600} units of MGM100 or MG1655 cells grown in LB medium containing arabinose or glucose for 5 h were used. The collected cells were ultrasonicated for 10 min, using a TOMY UD-201 (Tokyo, Japan). After centrifugation at 20,000 x g for 30 min, the proteins in the supernatant solution were reduced with 10 mM dithiothreitol for 30 min, alkylated with 55 mM iodoacetamide for 30 min at room temperature, and digested with trypsin. The digested sample was desalted with a C18-StageTip (Rappsilber et al, 2007) for the subsequent LC-MS analyses using an LTQ-Orbitrap XL (Thermo Fisher Scientific, Bremen, Germany) equipped with a Dionex Ultimate3000 pump (Germering, Germany) and an HTC-PAL autosampler (CTC Analytics, Zwingen, Switzerland). Details of the LC-MS conditions as well as the protein identification were described previously (Iwasaki et al, 2009; Masuda et al, 2009). Protein abundance based on emPAI was calculated according to the methods described previously (Ishihama et al, 2005).

Metabolomics

The methods basically followed those described previously (Soga & Heiger, 2000; Soga et al, 2007; Soga et al, 2003; Soga et al, 2002). In total, 20 OD_{600} units of MGM100 or MG1655 cells grown in LB medium containing arabinose or glucose at 5 h were used. An aliquot containing 20 OD_{600} units of cells was passed through a 0.45-μm pore size filter (Durapore HVLP09050, Millipore). To wash the cells, 10 ml portions of Milli-Q water were passed through the filter twice. The filter was plunged into 5 ml of methanol containing internal standards (2 μM each of 2-*N*-morpholino-ethanesulfonic acid, methionine sulfone and β-camphorsulfonic acid), sonicated for 30 sec. in a BRANSON 2200 sonicator, and incubated for 10 min. Chloroform (4 mL) and 1.6 ml of Milli-Q water were added to the solution and then thoroughly mixed. The 4 ml water layer was isolated after centrifugation and filtered through a Millipore 5-kDa-cutoff filter, to remove the high molecular weight molecules. The filtrate was lyophilized and dissolved in 50 μl of Milli-Q water containing a migration time standard, prior to analysis by CE-MS. Detailed conditions of analyses are available (Ishii et al, 2007).

SuhB assay

SuhB activity was determined by the malachite green method, as described (Chen & Roberts, 2000). A 1 μl aliquot of 10 mM inositol-1-phosphate (SiChem), was mixed with 1 μl of 200 mM $MgCl_2$, and 23 μl of 0.4 OD_{600} /ml cell lysate and the mixture was incubated for 2 min at 37 °C. Released phosphates were measured by the malachite-green method. Due to the increased PhoA activity in GroEL/GroES (GroE)-depleted cells (data not shown), both GroE-sufficient and -depleted cells without SuhB-inducible plasmids were used as controls. IPTG induction did not alter

the PhoA activity (data not shown). PhoA activity was detected by pNPP methods. Briefly, 10 µl of pNPP solution (WAKO), 180 µl STE buffer and 10 µl of 0.4 OD_{600} /ml cell lysate were mixed, and then incubated at 37 °C, after which Abs_{405} was measured. pNPP is reportedly not a substrate of SuhB (Chen & Roberts, 2000).

TrmD assay

TrmD activity was analyzed by the method described previously (Hjalmarsson et al, 1983). Purified tRNA(CAG) synthesized *in vitro* was used as the substrate. Cell lysates (6.8×10^{-3} OD_{600} unit) were added to a mixture containing 20 µM tRNA(CAG), 50 mM Hepes-KOH (pH 7.6), 100 mM 2-oxoglutamate, 2 mM spermidine, 13 mM $Mg(OAc)_2$, 1 mM DTT, 50 µM unlabeled *S*-adenosylmethionine (SAM, SIGMA), and ^3H SAM (37 MBq/ml), and incubated at 37 °C. An 8 µl aliquot of the reaction mixture was removed at 2, 4, 6, and 8 min and spotted onto blotting paper (Whatman 3MM CHR), which was immediately placed in a 10% trichloroacetic acid (TCA) solution to stop the reaction. After 2x30 min washes with 10% TCA, the papers were dried and the ^3H levels were quantified by liquid scintillation counting (ALOKA).

MetK

S-adenosylmethionine synthetase activity was assayed using a standard protocol (Markham et al, 1980). Cell lysates were added to an assay mixture containing 100 mM Tris-HCl (pH 8.3), 100 mM KCl, 20 mM $MgCl_2$, 10 mM ATP, and 1.2 mM L-[methyl-^{14}C] methionine (55 mCi/mmol; ARC). After 1, 2, and 3 min, aliquots of the mixtures were spotted onto P81 nitrocellulose paper (Whatman), and then washed with MilliQ water. ^{14}C levels were quantified by liquid scintillation counting (ALOKA).

***In vitro* translation using the reconstituted cell-free translation system (PURE system).**

FolE, DapA, SerC, and KdsA were synthesized by transcription-translation-coupled reconstituted cell-free translation for 2 h at 37 °C. The solubility of the synthesized protein was evaluated after centrifugation, as described previously (Fujiwara & Taguchi, 2007). The concentrations of the chaperones, which were a kind gift from Tatsuya Niwa, were as follows: 1 μM GroEL, 1 μM GroES, 4 μM DnaK, 2 μM DnaJ, and 2 μM GrpE. The products were radiolabeled with 0.1 MBq of [^{35}S] methionine and then were analyzed by SDS-PAGE or native PAGE. Proteins were detected with an FLA3000 imager (FUJIFILM).

Complementation assay for MetE overexpression

MGM100 cells harboring the plasmids encoding *Ureaplasma* MetK (pUuMetK) or *E. coli* MetK (pEcMetK) were precultivated to an early log phase by the same procedure described above, and then were inoculated into LB medium supplemented with 1 mM DAP, 200 μg/ml ampicillin, and 0.2 % arabinose or 0.2 % glucose. After overnight cultivation, the cells were collected. Total lysates were obtained by sonication and were analyzed by SDS-PAGE.

Supplemental references

Baba T, Ara T, Hasegawa M, Takai Y, Okumura Y, Baba M, Datsenko KA, Tomita M, Wanner BL, Mori H (2006) Construction of Escherichia coli K-12 in-frame, single-gene knockout mutants: the Keio collection. Mol Syst Biol 2: 2006 0008

Chapman E, Farr GW, Usaite R, Furtak K, Fenton WA, Chaudhuri TK, Hondorp ER, Matthews RG, Wolf SG, Yates JR, Pypaert M, Horwich AL (2006) Global aggregation of newly translated proteins in an Escherichia coli strain deficient of the chaperonin GroEL. Proc Natl Acad Sci U S A 103: 15800-15805

Chen L, Roberts MF (2000) Overexpression, purification, and analysis of complementation behavior of E. coli SuhB protein: comparison with bacterial and archaeal inositol monophosphatases. Biochemistry 39: 4145-4153

Fujiwara K, Taguchi H (2007) Filamentous morphology in GroE-depleted Escherichia coli induced by impaired folding of FtsE. J Bacteriol 189: 5860-5866

Hjalmarsson KJ, Bystrom AS, Bjork GR (1983) Purification and characterization of transfer RNA (guanine-1)methyltransferase from Escherichia coli. J Biol Chem 258: 1343-1351

Ishihama Y, Oda Y, Tabata T, Sato T, Nagasu T, Rappsilber J, Mann M (2005) Exponentially modified protein abundance index (emPAI) for estimation of absolute protein amount in proteomics by the number of sequenced peptides per protein. Mol Cell Proteomics 4: 1265-1272

Ishii N et al (2007) Multiple high-throughput analyses monitor the response of E. coli to perturbations. Science 316: 593-597

Iwasaki M, Masuda T, Tomita M, Ishihama Y (2009) Chemical cleavage-assisted tryptic digestion for membrane proteome analysis. J Proteome Res 8: 3169-3175

Kerner MJ, Naylor DJ, Ishihama Y, Maier T, Chang HC, Stines AP, Georgopoulos C, Frishman D, Hayer-Hartl M, Mann M, Hartl FU (2005) Proteome-wide analysis of chaperonin-dependent protein folding in Escherichia coli. Cell 122: 209-220

Kyte J, Doolittle RF (1982) A simple method for displaying the hydropathic character of a protein. J Mol Biol 157: 105-132

Markham GD, Hafner EW, Tabor CW, Tabor H (1980) S-Adenosylmethionine synthetase from Escherichia coli. J Biol Chem 255: 9082-9092

Masuda T, Saito N, Tomita M, Ishihama Y (2009) Unbiased quantitation of Escherichia coli membrane proteome using phase transfer surfactants. Mol Cell Proteomics 8: 2770-2777

McLennan N, Masters M (1998) GroE is vital for cell-wall synthesis. Nature 392: 139

Mourino S, Osorio CR, Lemos ML (2004) Characterization of heme uptake cluster genes in the fish pathogen Vibrio anguillarum. J Bacteriol 186: 6159-6167

Niwa T, Ying BW, Saito K, Jin W, Takada S, Ueda T, Taguchi H (2009) Bimodal protein solubility distribution revealed by an aggregation analysis of the entire ensemble of Escherichia coli proteins. Proc Natl Acad Sci U S A 106: 4201-4206

Rappsilber J, Mann M, Ishihama Y (2007) Protocol for micro-purification, enrichment, pre-fractionation and storage of peptides for proteomics using StageTips. Nat Protoc 2: 1896-1906

Reddy M (2007) Role of FtsEX in cell division of Escherichia coli: viability of ftsEX mutants is dependent on functional SufI or high osmotic strength. J Bacteriol 189: 98-108

Soga T, Heiger DN (2000) Amino acid analysis by capillary electrophoresis electrospray ionization mass spectrometry. Anal Chem 72: 1236-1241

Soga T, Ishikawa T, Igarashi S, Sugawara K, Kakazu Y, Tomita M (2007) Analysis of nucleotides by pressure-assisted capillary electrophoresis-mass spectrometry using silanol mask technique. J Chromatogr A 1159: 125-133

Soga T, Ohashi Y, Ueno Y, Naraoka H, Tomita M, Nishioka T (2003) Quantitative metabolome analysis using capillary electrophoresis mass spectrometry. J Proteome Res 2: 488-494

Soga T, Ueno Y, Naraoka H, Ohashi Y, Tomita M, Nishioka T (2002) Simultaneous determination of anionic intermediates for Bacillus subtilis metabolic pathways by capillary electrophoresis electrospray ionization mass spectrometry. Anal Chem 74: 2233-2239

Supplemental tables

Table S1. Accumulated and decreased metabolites in GroE-depleted cells

Accumulated metabolites (μM)	MGM100		MG1655	
	Ara	Glc	Ara	Glc
Cadaverine	0.1	31.2	1.2	7.8
N-Acetylputrescine	15.5	43.9	3.5	5.9
5-Aminolevulinate	0.4	38.1	1.5	1.5
Adenine	14.2	97.8	7.7	20.8
Pterin	3.5	18.5	4.2	3.3
N-Acetylornithine	0.7	7.6	1.0	1.6
*N*8-Acetylspermidine	0.7	6.4	1.4	2.9
Cytidine	0.8	2.3	0.8	0.7
Thiamine monophosphate	N.D.	9.5	N.D.	N.D.

Decreased metabolites (μM)	MGM100		MG1655	
	Ara	Glc	Ara	Glc
Trimethylamine *N*-oxide	0.9	0.4	1.4	1.6
Cyclohexanecarboxylate	1.5	0.3	0.6	1.6
Lys	293	44.0	417	559
O-Phosphoserine	2.5	N.D.	4.4	0.5
N-Acetylglutamate	1.1	0.5	7.7	6.1
Citrate	10.9	2.8	22.4	19.4
S-Adenosylmethionine	85.4	2.2	83.8	85.2
2-Deoxyribose 1-phosphate	1.5	0.5	1.0	1.3
N-Acetylglucosamine	5.7	2.2	7.9	8.6
Glycerophosphorylcholine	12.5	1.8	5.2	5.6
Inosine	6.1	0.2	1.9	15.5
Sedoheptulose 7-phosphate	22.5	8.7	36.8	19.4
N-Acetylmuramate	3.6	N.D.	8.5	10.6
5-Methylthioadenosine	1.9	N.D.	1.8	1.3
N-Acetylglucosamine 1-phosphate	6.9	1.8	7.4	8.3
dCMP	6.0	2.3	5.8	8.0
UMP	63.9	25.1	52.1	60.9
AMP	357	88.1	232	240
NADPH	12.6	0.6	11.2	1.6
GDP	108	34.4	109	107

N.D.: not detected

Table S2. Class III⁻ substrates

gene	b num	ES[a]	Sol[b]	MW[c]	A/G[d]	R/K/H[e]	pI	folds[f]	function
ybaK	b0481	0	100%	17079	20.8%	15.7%	9.0	d.116	Cys-tRNAPro and Cys-tRNACys deacylase
hlpA	b0178	0	26%	17675	18.6%	16.1%	9.5	OmpH-like	periplasmic chaperone
rsd	b3995	0	93%	18223	12.7%	15.2%	5.7		stationary phase protein, binds sigma 70 RNA polymerase subunit
smpB	b2620	0	101%	18266	16.9%	22.5%	9.9	b.111	trans-translation protein
ubiC	b4039	0	66%	18777	11.5%	13.3%	7.7	d.190	chorismate pyruvate lyase
ycfP	b1108	0	24%	21207	7.8%	17.8%	6.1		conserved protein
rimJ	b1066	0	n.d.	22676	15.5%	18.0%	9.2	d.108	ribosomal-protein-S5-alanine N-acetyltransferase
yqjI	b3071	0	61%	23384	16.4%	19.8%	6.3		predicted transcriptional regulator
crp	b3357	0	n.d.	23670	13.8%	15.7%	8.4	b.82; a.4	DNA-binding transcriptional dual regulator
folE	b2153	1	50%	24811	12.2%	15.3%	6.9	d.96	GTP cyclohydrolase I
trmI	b2960	0	40%	27284	13.8%	17.2%	6.4	c.66	tRNA (m7G46) methyltransferase, SAM-dependent
pflA	b0902	0	95%	28177	13.0%	17.1%	6.0	c.7	pyruvate formate lyase activating enzyme 1
trmD	b2607	1	30%	28390	17.6%	14.1%	5.5	c.116	tRNA (guanine-1-)-methyltransferase
glcC	b2980	0	20%	28810	12.6%	18.1%	9.2	a.4	DNA-binding transcriptional dual regulator, glycolate-binding
suhB	b2533	1	87%	29142	21.0%	13.1%	6.5	e.7	inositol monophosphatase
amiA	b2435	0	37%	31408	18.0%	20.1%	9.9		N-acetylmuramoyl-l-alanine amidase I
yhbJ	b3205	0	39%	32462	10.6%	16.2%	6.7	c.37	predicted protein with nucleoside triphosphate hydrolase domain
araC	b0064	0	28%	33355	14.4%	14.0%	6.5	b.82; a.4	DNA-binding transcriptional dual regulator
yceC	b1086	0	63%	36011	15.4%	20.7%	9.9	d.66; d.58	23S rRNA pseudouridylate synthase
yfiF	b2581	0	81%	37755	19.7%	16.8%	8.9	c.116	RNA methyltransferase, TrmH family
hisB	b2022	0	67%	40235	13.8%	15.5%	5.8	c.108	fused histidinol-phosphatase/imidazoleglycerol-phosphate dehydratase

ybeZ	b0660	0	62%	40612	15.0%	16.2%	5.7		predicted protein with nucleoside triphosphate hydrolase domain
dnaJ	b0015	0	52%	41066	21.3%	16.8%	8.0	a.2; b.49; a.4; a.138; g.54	chaperone Hsp40, co-chaperone with DnaK
trmA	b3965	0	42%	41921	12.3%	13.7%	5.7		tRNA (uracil-5-)-methyltransferase
rlmG	b3084	0	57%	42291	14.0%	13.8%	6.3	c.66	23S rRNA m2G1835 methyltransferase
pheA	b2599	0	44%	43071	14.5%	13.7%	6.2	a.130; d.58	fused chorismate mutase P/prephenate dehydratase
intS	b2349	0	59%	44030	14.5%	17.7%	9.4	d.163	CPS-53 (KpLE1) prophage; predicted prophage CPS-53 integrase
gatZ	b2095	0	7%	47055	16.4%	12.6%	5.6	c.1	D-tagatose 1,6-bisphosphate aldolase 2, subunit
rhlE	b0797	0	63%	49966	18.9%	18.7%	10.1	c.37	RNA helicase
pepA	b4260	0	58%	54826	19.3%	13.1%	6.8	c.50; c.56	aminopeptidase A, a cysteinylglycinase
deaD	b3162	0	50%	70478	17.8%	17.2%	8.8	c.37	ATP-dependent RNA helicase
rlmL	b0948	0	22%	78790	17.2%	15.2%	9.0	c.66	23S rRNA m2G2445 methyltransferase
parC	b3019	0	18%	83743	15.4%	14.9%	6.2	e.11	DNA topoisomerase IV, subunit A
malP	b3417	0	n.d.	90520	16.2%	14.9%	6.9	c.87	maltodextrin phosphorylase

a; essentiality of the gene (Baba et al, 2006). 1 and 0 indicate essential and nonessential, respectively.

b; solubility when synthesized in a reconstituted cell-free translation system without any chaperone (Niwa et al, 2009)

c: molecular weight (Da)

d; content of alanine and glycine

e; content of positively charged amino acids

f; SCOP fold ID of the proteins

n.d.: not determined in (Niwa et al, 2009)

Supplemental Figures

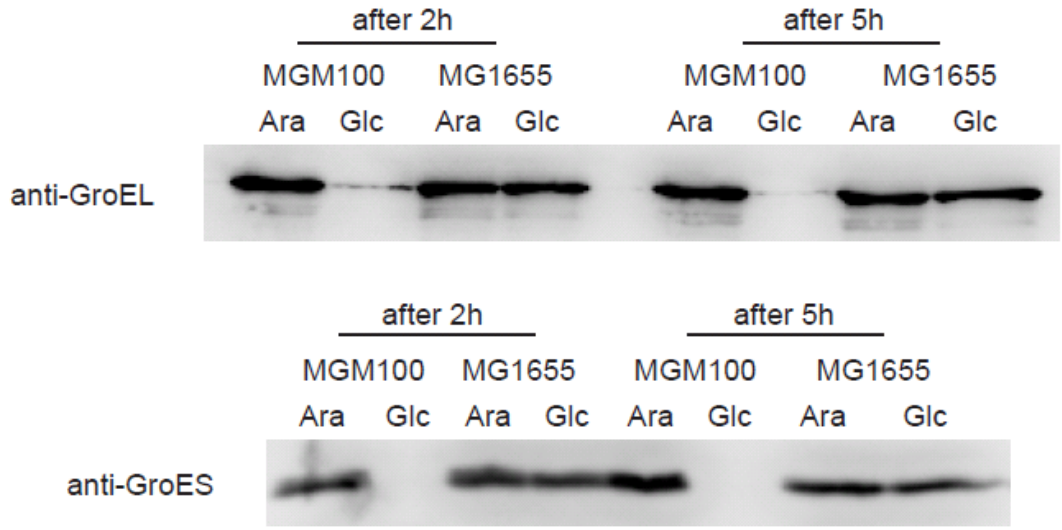

Supplemental Figure S1. Expression levels of GroEL and GroES in MGM100 and the wild-type parent MG1655 cells after the sugar shift from arabinose (*Ara*) to glucose (*Glc)*.

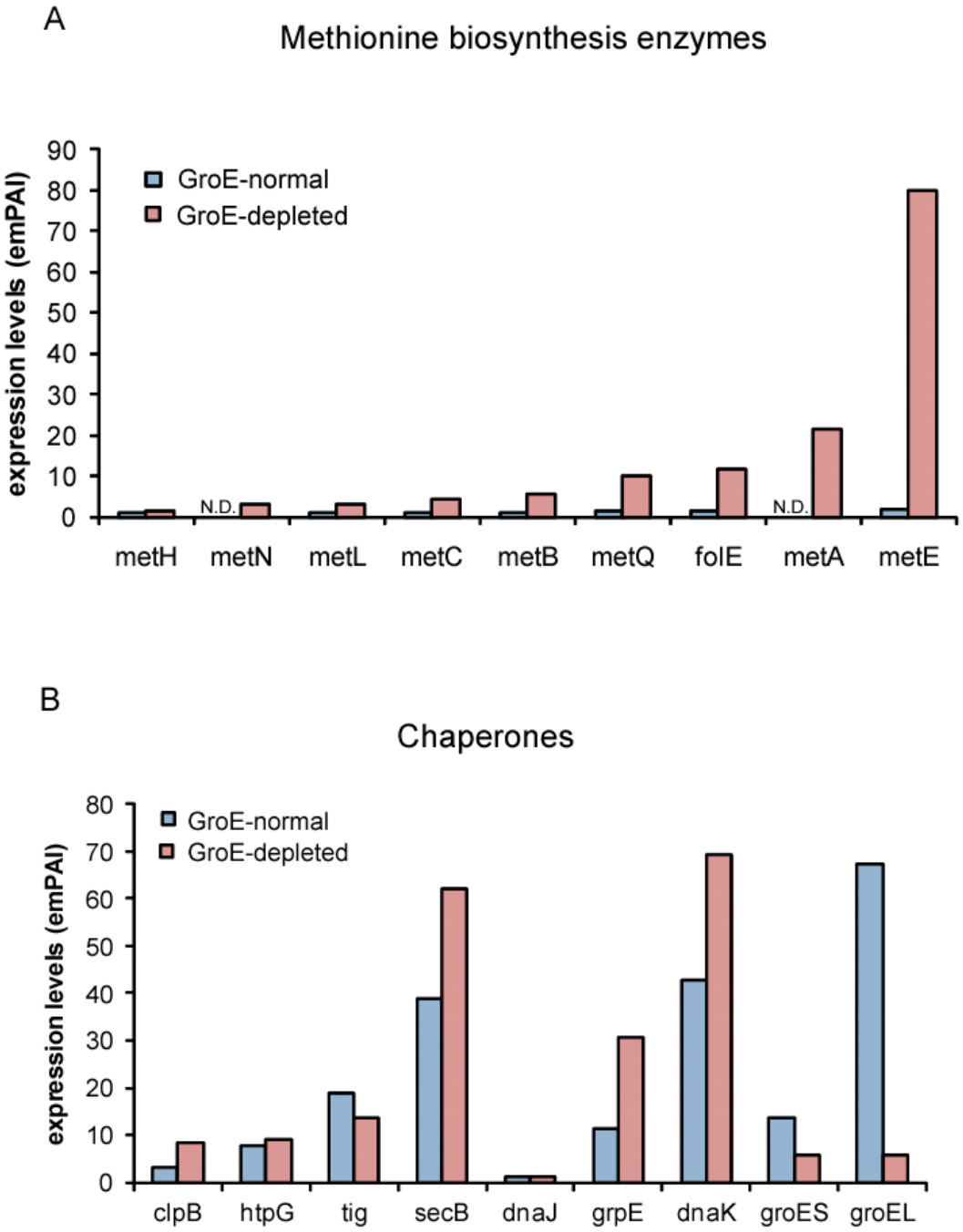

Supplemental Figure S2.
The emPAI-based expression levels of methionine biosynthesis enzymes (A) and chaperones (B) in GroE-normal (blue) and -depleted (red) cells.

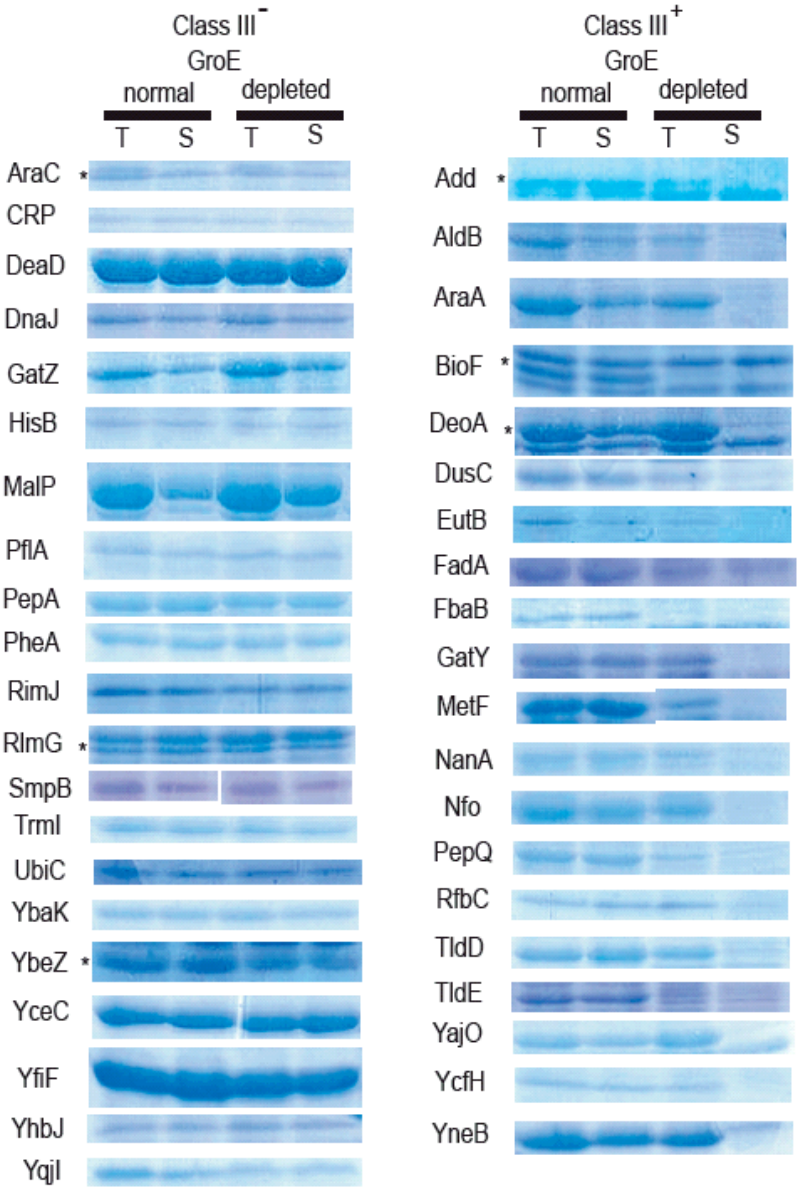

Supplemental Figure S3. Solubilities of Class III substrates after overexpression in GroE-normal and -depleted cells. Proteins were stained with Coomassie Brilliant Blue. Asterisks indicate the bands of expressed proteins where necessary.

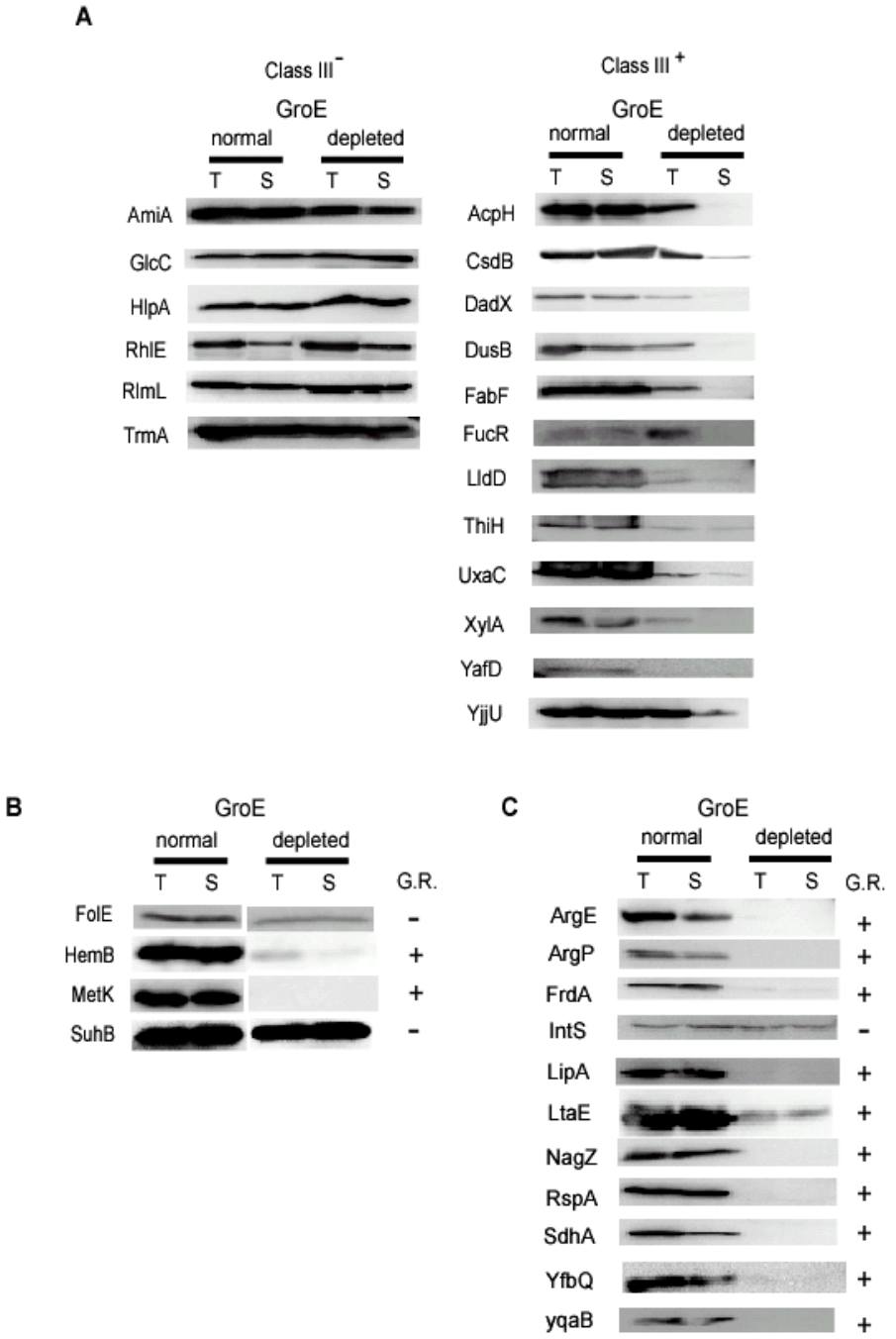

Supplemental Figure S4. Assessments of GroE dependency by immunoblotting. (A) Proteins, for which the expression could not be detected by CBB, were HA-tagged at their C-termini. Solubilities of the HA-tagged Class III substrates after overexpression in normal and depleted cells are shown. (B) Several Class III substrates previously assessed after overexpression (Fig. 2) were verified here to show the same behavior when immuno-tagged and uninduced (leaky expression was used). Cells were collected at 5 h after the sugar shift. (C) Among the Class III substrates evaluated by the leaky expression method, all except IntS were GroE-dependent. G.R.: GroE requirement.

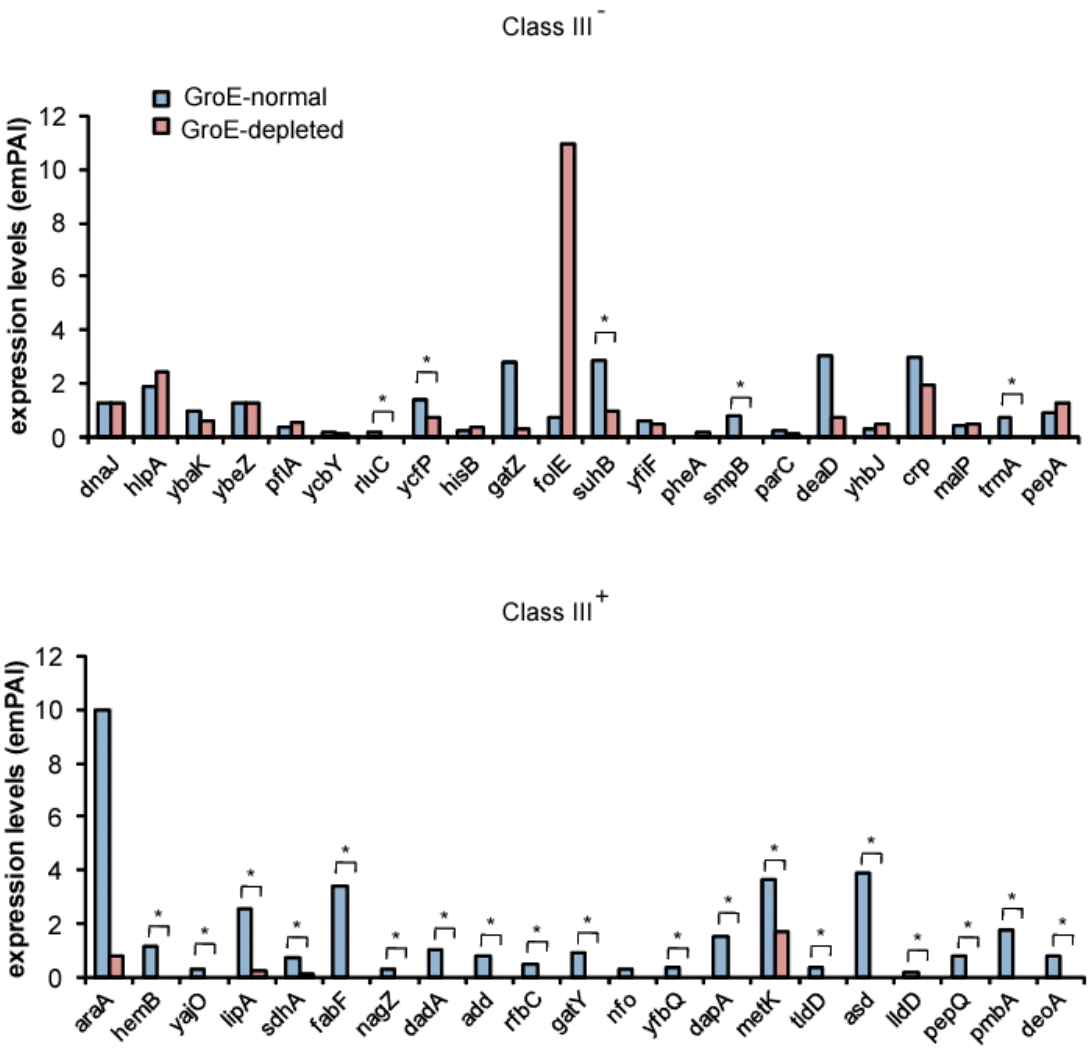

Supplemental Figure S5. Expression levels of Class III^{-} and III^{+} proteins in GroE-normal cells (blue) and -depleted cells (red) measured by proteomics. Asterisks show the proteins with significantly reduced abundance in GroE-depleted cells. Significance was judged as described in the legend of Fig. 1C. Note that AraA is known to be induced by arabinose and repressed by glucose.

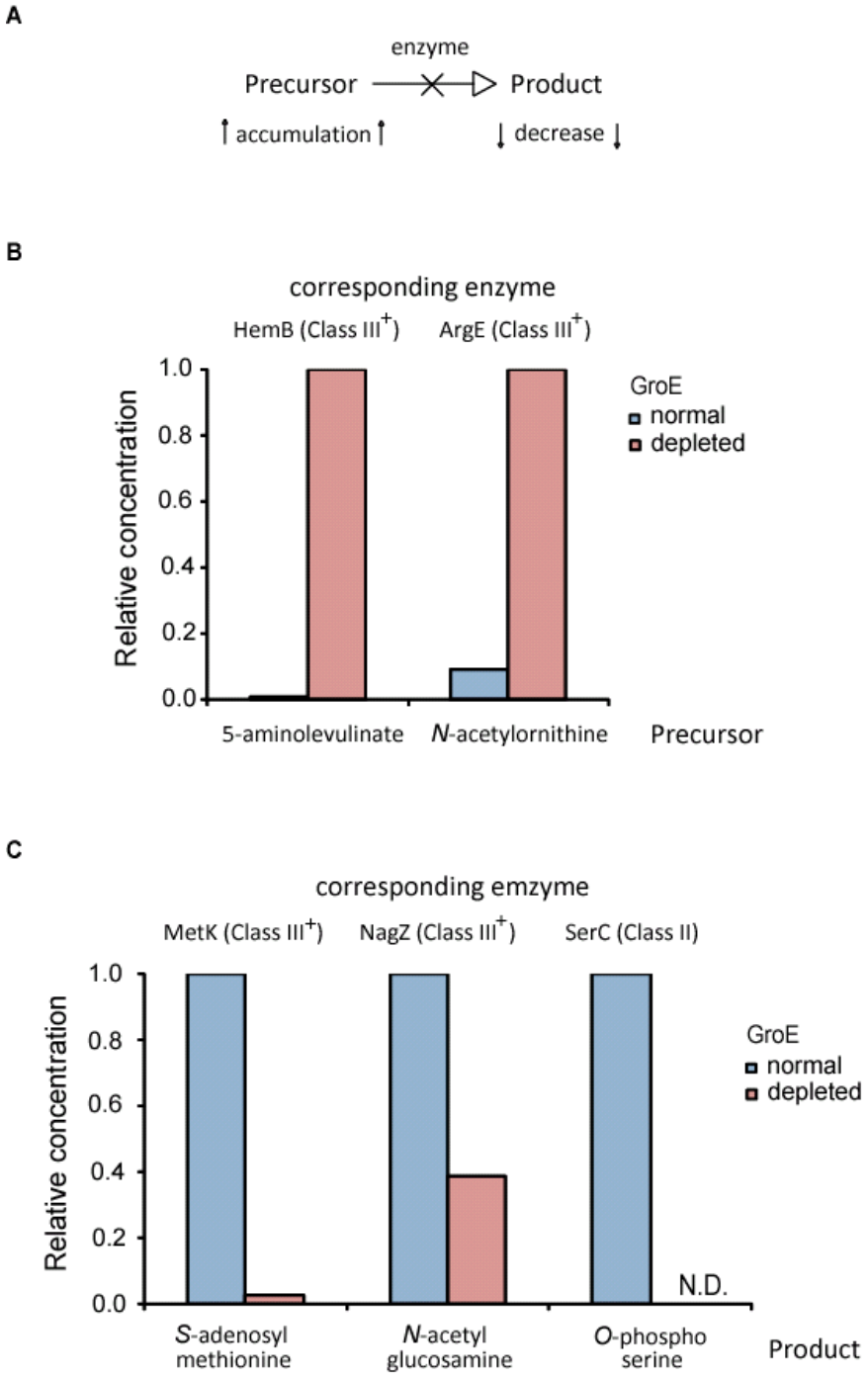

Supplemental Figure S6. (A) Lack of active enzyme leads to the accumulation of precursor and/or the reduction of product. (B) Concentrations of 5-aminolevulinate and *N*-acetylornithine, which are the precursors of the reactions catalyzed by the Class III^{+} (IV) substrates HemB and ArgE, respectively, accumulated in GroE-depleted cells. (C) Concentrations of *S*-adenosylmethionine, acetylglucosamine, and *O*-phosphoserine, which are the products of the reactions catalyzed by the Class III^{+} (IV) substrates MetK and NagZ, and a Class II substrate, SerC, respectively, were decreased in GroE-depleted cells.

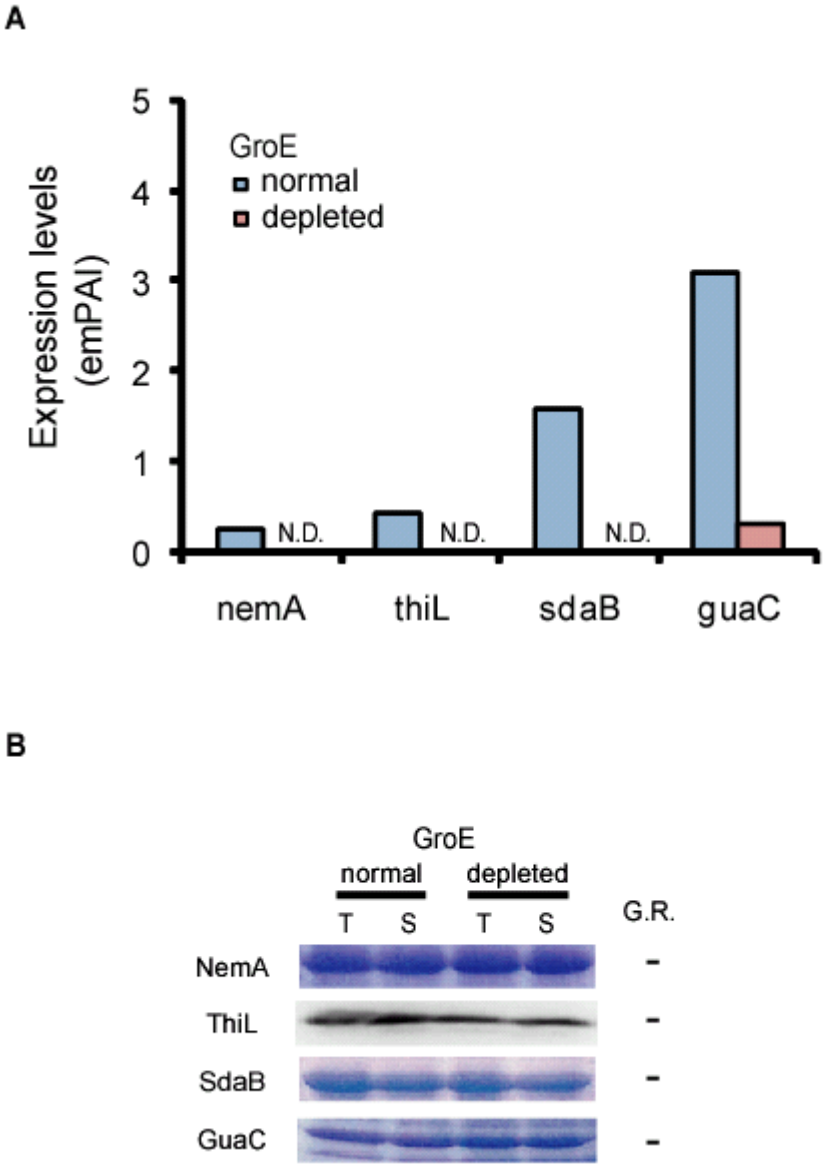

Supplemental Figure S7. (A) Expression levels of several proteins that had not been identified as GroEL substrates in GroE-normal cells (*blue*) and -depleted cells (*red*). Several proteins that were specifically reduced in GroE-depleted cells were chosen as candidates to evaluate the GroE dependency, as shown in (B). Expression levels are represented by the emPAI values. *N.D.*: significant expression of the proteins was not detected. (B) Solubility of the candidate GroE substrates in GroE-depleted cells. All proteins were stained by Coomassie Brilliant Blue, except for ThiL, which was detected by immunoblotting with HA-tagged ThiL. *G.R.*: GroE requirement.

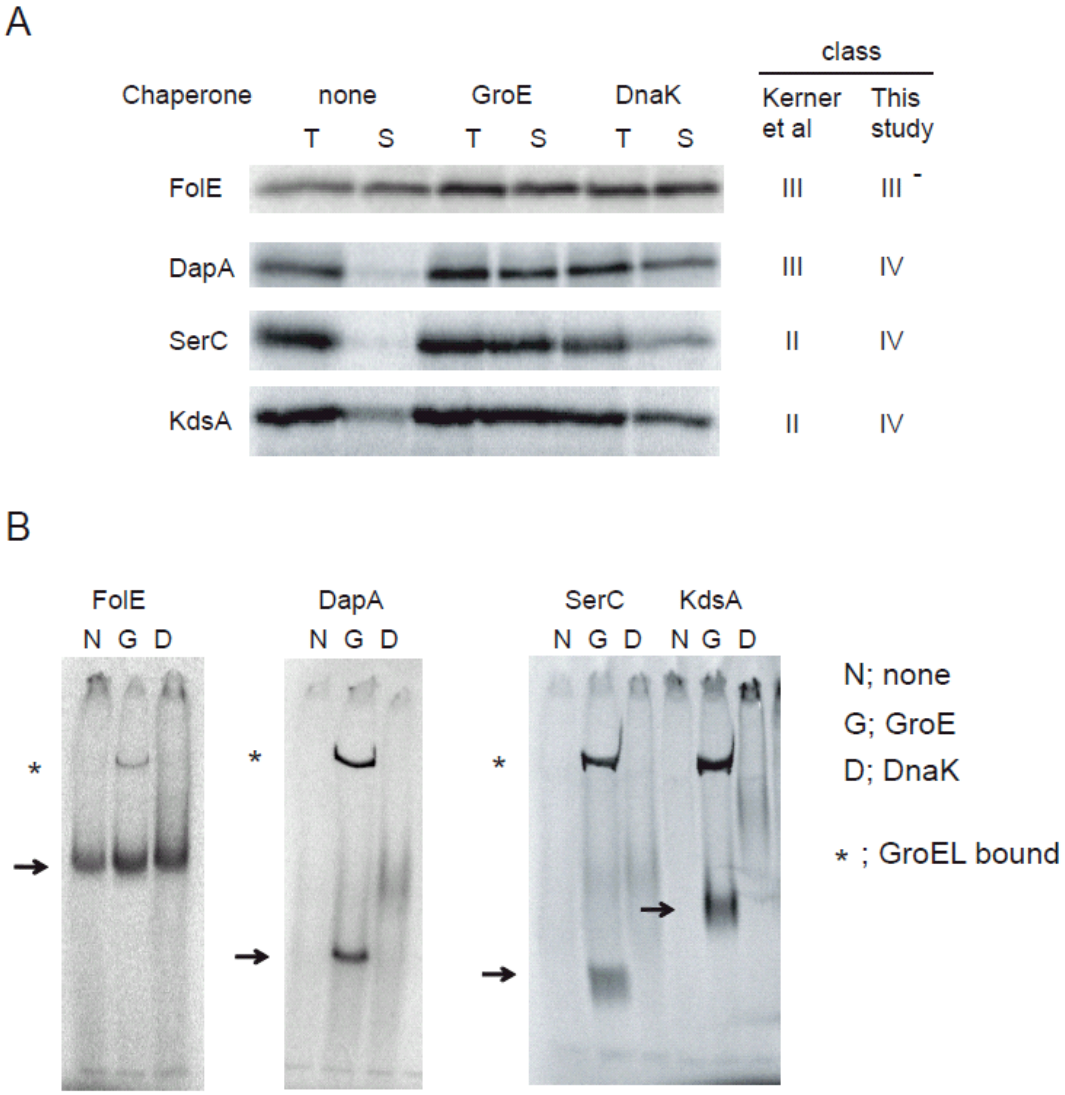

Supplemental Figure S8. GroE dependency of several Class IV and III^{-} substrates in reconstituted cell-free translation (PURE system). (A) Effects of chaperones on the solubility of nascent proteins translated by PURE system. FolE, DapA, SerC, and KdsA were synthesized by the PURE system in the absence or presence of chaperones (GroE: GroEL and GroES; DnaK: DnaK, DnaJ and GrpE). The total fraction (T) and the soluble fraction (S) after centrifugation of the translation mixtures were subjected to SDS-PAGE, followed by autoradiography. Only the regions of the synthesized proteins are shown. (B) Native PAGE analysis of the cell-free translated proteins. Arrows and asterisks indicate folded structures defined as a sharp band, and GroEL-bound proteins, respectively. Synthesized proteins that contained [^{35}S] methionine were detected by autoradiography.

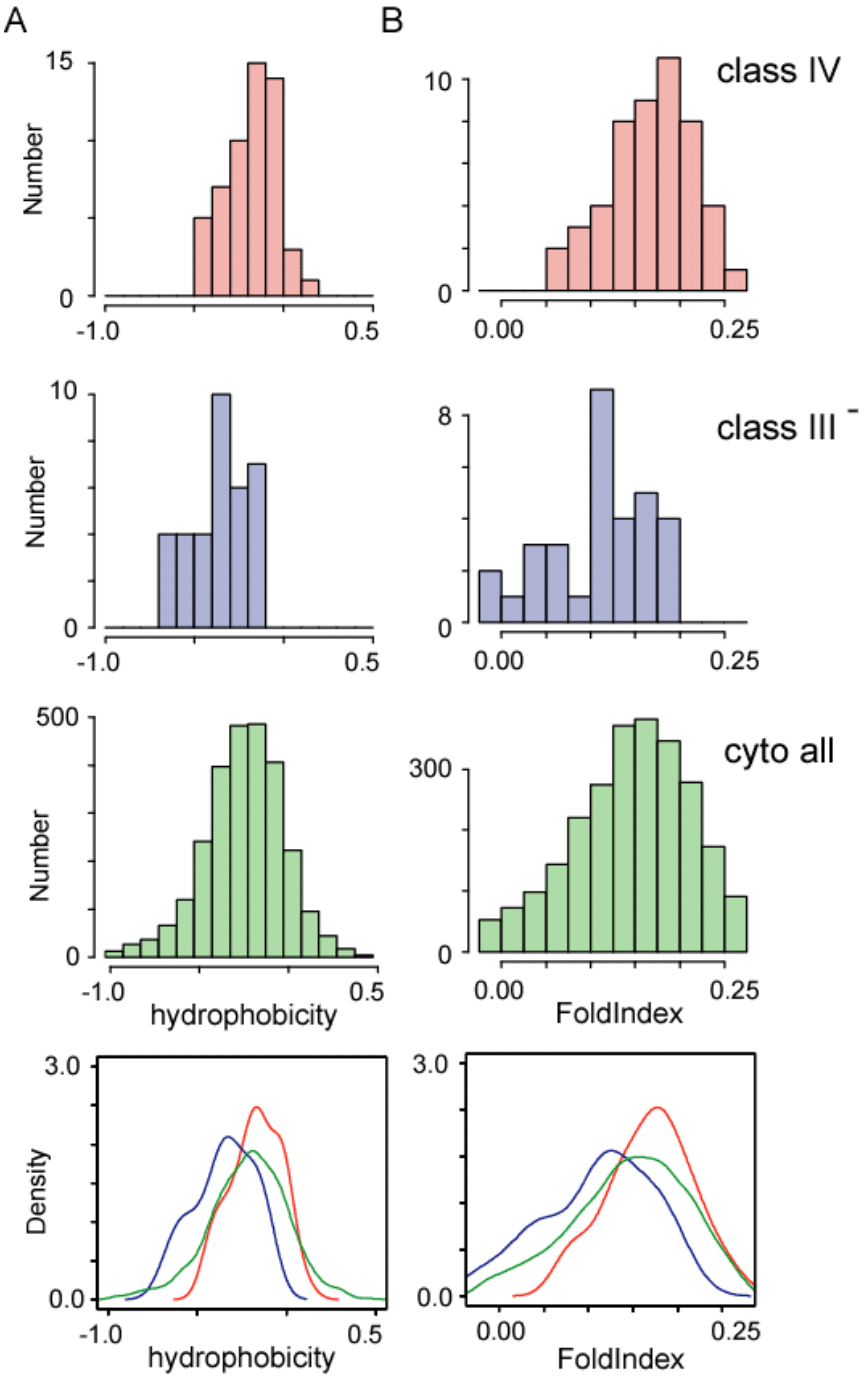

Supplemental Figure S9. (A) The hydrophobicity distribution of Class III⁻ and IV proteins. Hydrophobicities were calculated by the Kyte-Doolittle method (Kyte & Doolittle, 1982). (B) The FoldIndex distribution of Class III⁻ and IV proteins. FoldIndex was calculated according to http://bioportal.weizmann.ac.il/fldbin/findex. In each figure, the bottom graphs show the hydrophobicity properties as Kernel type density maps for Class IV (*red*), III⁻ (*blue*), and all *E. coli* cytosolic proteins (*green*).

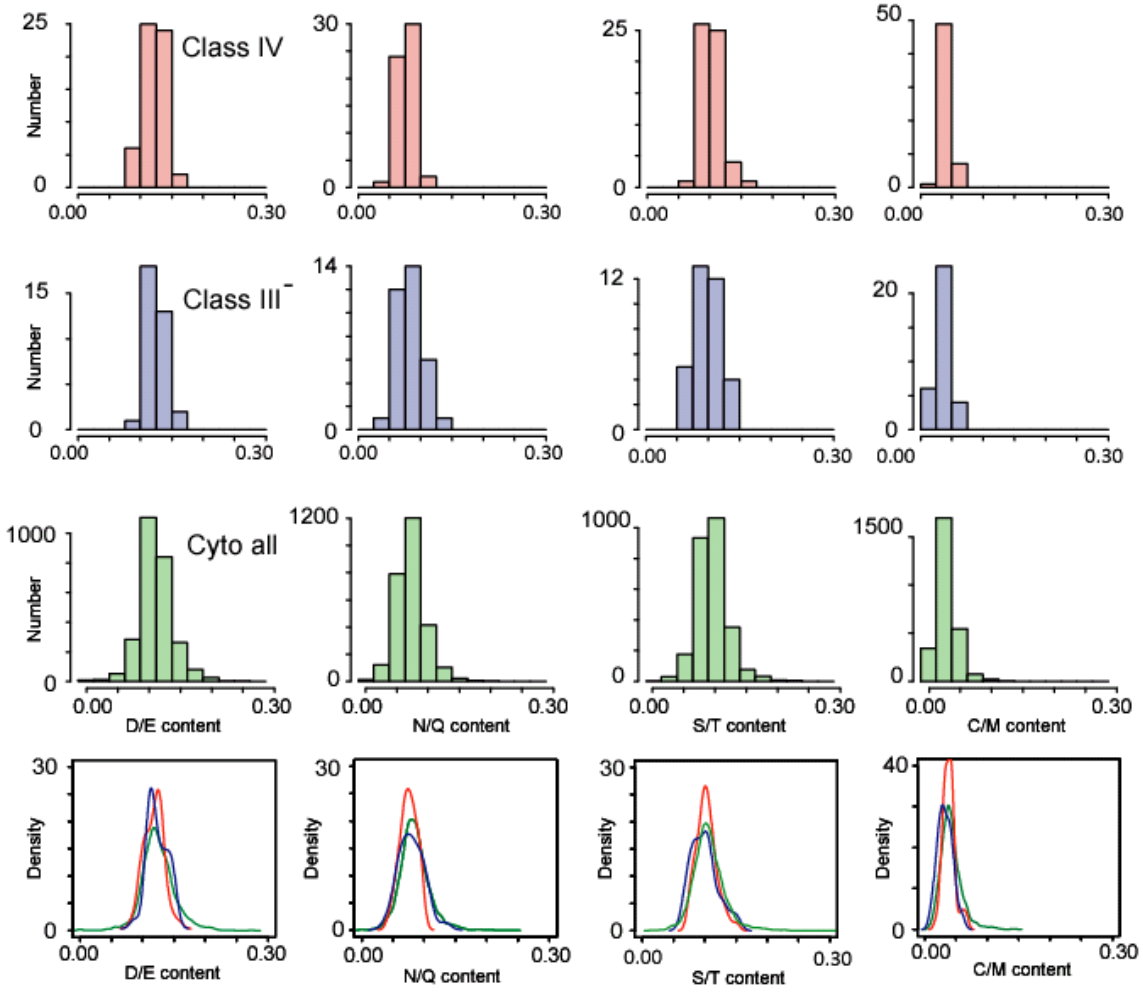

Supplemental Figure S10. The distributions of amino acid compositions in Class III⁻ and IV proteins. The bottom graphs show the compositions as Kernel type density maps for the amino acid compositions of Class IV (red), Class III⁻ (blue), and all *E. coli* cytosolic proteins (green). D/E, aspartate and glutamate (negatively charged); N/Q, asparagine and glutamine; S/T, serine and threonine (neutral); C/M, cysteine and methionine (sulfur containing).

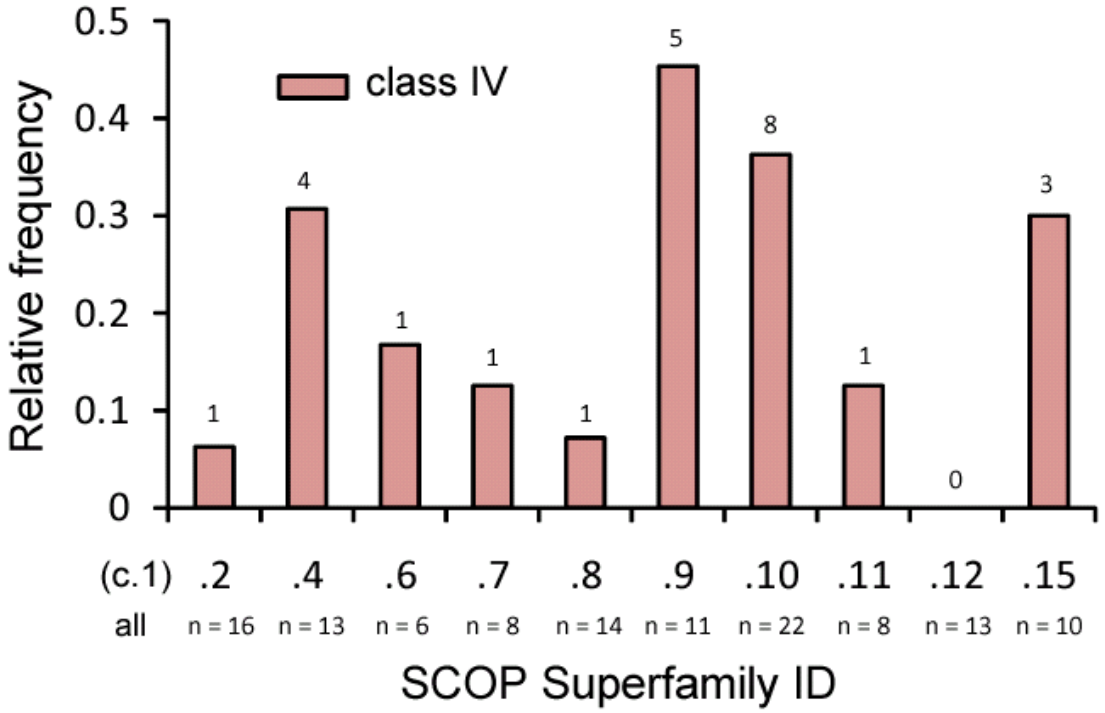

Supplemental Figure S11. Relative frequencies of Class IV substrates in the TIM barrel superfamily. Only the superfamilies with more than 6 proteins present in *E. coli* are shown. The number above each bar indicates the frequency of the fold among Class IV substrates. c.1.2, Ribulose-phosphate binding barrel (n = 16); c.1.4, FMN-linked oxidoreductases (n = 13); c.1.6, PLP-binding barrel (n = 6); c.1.7, NAD(P)-linked oxidoreductase (n = 8); c.1.8, (Trans) glycosidases (n = 14); c.1.9, Metallo-dependent hydrolases (n = 11); c.1.10, Aldolase (n = 22); c.1.11, Enolase C-terminal domain-like (n = 8); c.1.12, Phosphoenolpyruvate/pyruvate domain (n = 13); c.1.15, Xylose isomerase-like (n = 10).

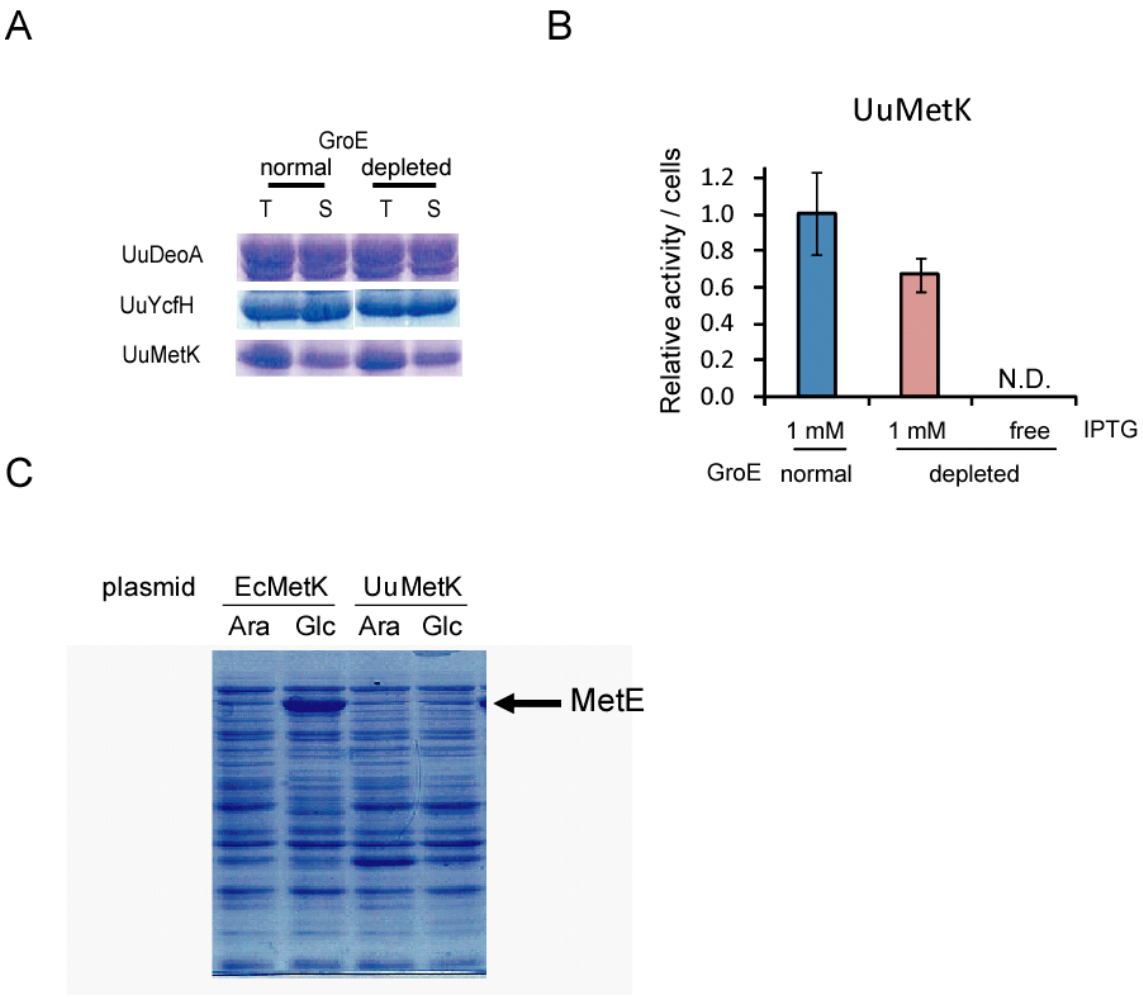

Supplemental Figure S12. (A) Solubilities of Class IV homologs from *Ureaplasma urealyticum* in GroE-depleted cells. *E. coli* MGM100 cells harboring *Uu*DeoA, *Uu*MetK and *Uu*YcfH were cultivated under arabinose or glucose conditions. Homologs were induced with IPTG 2 h after the sugar shift, After 3 h, cells were collected. Whole lysates were fractionated by SDS-PAGE, and were stained by Coomassie Brilliant Blue. (B) Enzymatic activities of *Uu*MetK in *E. coli* lysates. MGM100 cells harboring IPTG-inducible plasmids for *Uu*MetK were grown under GroE-normal or –depleted conditions, in the presence or absence of IPTG. Relative SAM synthase activity is shown. (C) The overexpression of MetE in GroE-depleted cells was suppressed by the expression of *Uu*MetK. It has been shown that the impairment of MetK function leads to the overexpression of MetE ((Chapman et al, 2006); Supplemental Figure S2A). *E. coli* MGM100 cells harboring MetK of *E. coli* (*Ec*MetK) or *Uu*MetK were cultivated under arabinose or glucose conditions without induction. Whole lysates were fractionated by SDS-PAGE and were stained by Coomassie Brilliant Blue.

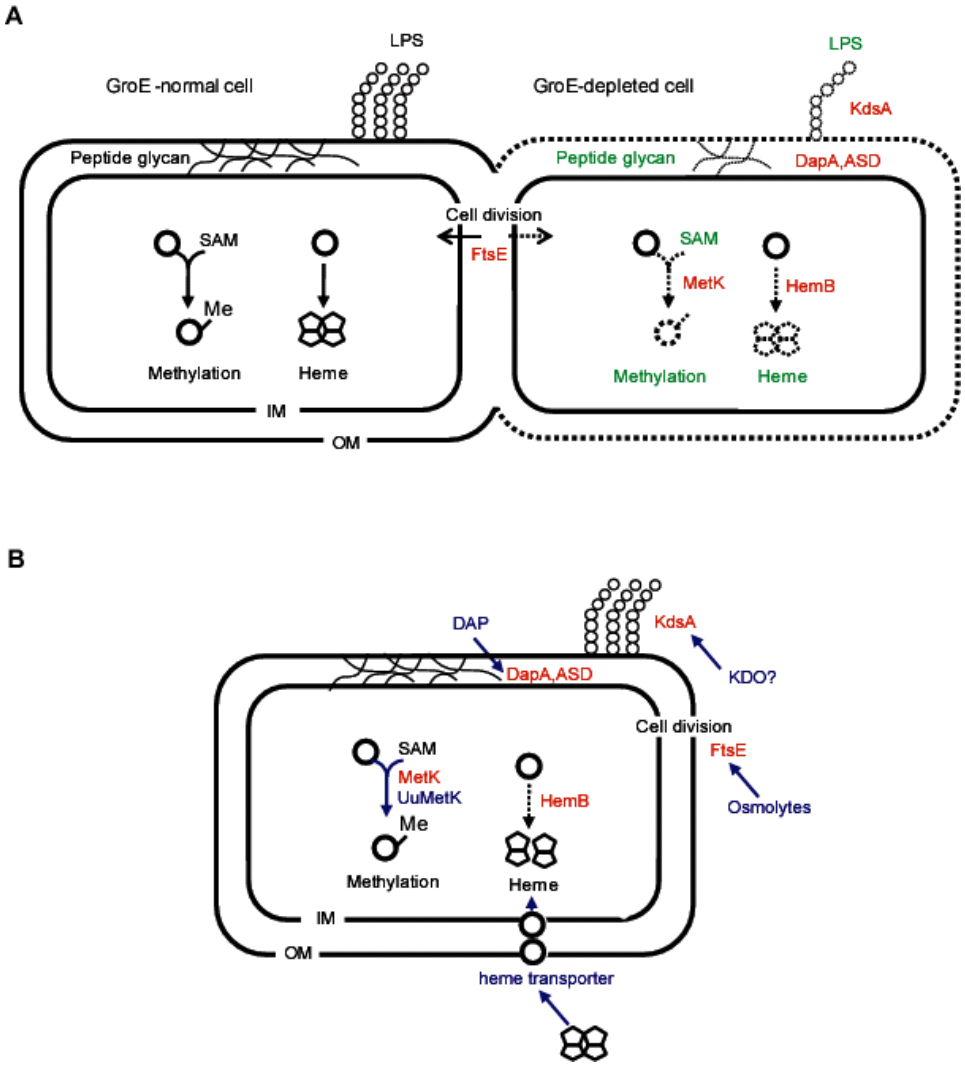

Supplemental Figure S13. Six essential proteins among the Class IV substrates. (A) Reactions involving the six essential Class IV substrates. Left and right cells indicate the GroE-normal and -depleted cells, respectively. MetK, SAM-deficiency (i.e. methylation-deficiency, as SAM is one of the most important substrates for methylation); HemB, heme-deficiency; KdsA, lipopolysaccharide (LPS)-deficiency; FtsE, defect of cell division; DapA/ASD, impairment of cell wall synthesis. (B) Possible complementation methods to rescue dysfunctions of the essential Class IV substrates in GroE-depleted cells. Blue characters indicate ways to rescue the dysfunctions of essential Class IV proteins. DapA and ASD are dispensable in rich medium supplemented with DAP (Fujiwara & Taguchi, 2007; McLennan & Masters, 1998). MetK of *Ureaplasma* is sufficient to complement the MetK-deficiency in GroE-depleted cells, as shown in this work (Fig. S12). High salt reportedly suppresses the FtsE-deficiency (Reddy, 2007). The introduction of a heme transporter gene from another organism might be worth testing to rescue the HemB-deficiency (Mourino et al, 2004). Regarding KdsA, as far as we know, no supplement or gene has been reported to rescue the deficiency, although supplying a downstream metabolite of the lipopolysaccharide biosynthesis pathway may circumvent the requirement for KdsA.

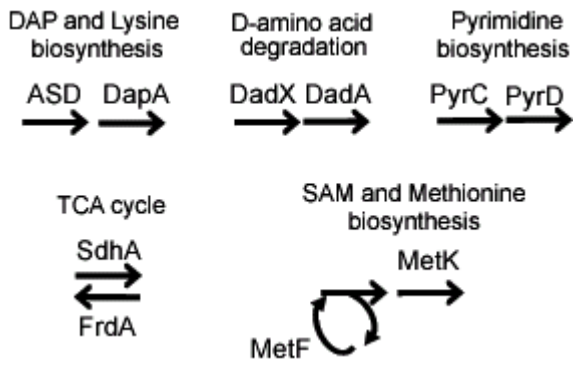

Supplemental Figure S14. The reactions of several pairs of Class IV substrates are closely linked in metabolic pathways. The reactions of MetK/MetF are coupled. The reactions of ASD/DapA, DadX/DadA, and PyrC/PyrD are sequential. The reaction of SdhA is the reverse of that of FrdA.